Int. J. Heat Mass Transfer. Vol. 10, pp. 83–95. Pergamon Press 1967. Printed in Great Britain

THE EFFECT OF WALL TEMPERATURE ON THE LOW REYNOLDS NUMBER HYPERSONIC STAGNATION REGION SHOCK LAYER

J. T. C. LIU†

Gas Dynamics Laboratory, Department of Aerospace and Mechanical Sciences, Princeton University, Princeton, New Jersey

(*Received* 27 *September* 1965 *and in revised form* 18 *March* 1966)

Abstract—The effect of wall temperature on the behavior of the hypersonic stagnation region shock layer in incipient merged layer flow is described. The enthalpy function profile across the shock layer is obtained. The shock detachment distance is shown to be subjected to the compensating corrections of an "inflow" effect due to velocity slip and an "outflow" effect due to temperature jump, with the main contribution coming from the over-all density decrease due to wall heating. The net corrections render the shock detachment distance to remain relatively constant with K^2 for a fixed wall temperature, where K^2 is the rarefaction parameter. The ratio of heat flux behind the shock wave to that at the wall is shown to be independent of the wall temperature and is essentially the same as the corresponding ratio when slip effects are absent.

NOMENCLATURE

a, nose radius;
C_H, heat-transfer coefficient;
c_p, specific heat at constant pressure;
f, nondimensional stream function $(f_\eta = u/u_\infty)$;
H, $c_pT + (u^2 + v^2)/2$, total specific enthalpy;
k, thermal conductivity; also $(2Pr/3)\{[4/K^2) + 1]^{\frac{1}{2}} - 1\}^{-1}$;
K^2, $(\epsilon\rho_\infty Ua/\mu_*)(T_*/T_0)$, rarefaction parameter;
Pr, $c_p\mu/k$, Prandtl number;
p, pressure;
$\dot{q}$, heat flux;
T, temperature;
U, free stream velocity;
u, v, velocity components tangential and normal to surface, respectively;
x, y, distance along and normal to body surface, respectively;
Z, distance from centerline to body surface;
α, thermal-accommodation coefficient;
β, local body surface inclination;
γ, c_p/c_v, ratio of specific heats;
$\gamma(a, \chi)$, $\int_0^\chi \exp(-t)\, t^{a-1}\, dt$, incomplete gamma function of order a and argument χ;
ϵ, $(\gamma - 1)/(\gamma + 1)$;
η, Howarth variable: transformed normal distance to body surface;
ξ, transformed tangential distance along body surface;
θ, $(H - H_w)/(H_\infty - H_w)$;
κ, longitudinal body surface curvature;
μ, viscosity;
ρ, density;
σ, Maxwell's reflection coefficient;
ψ, stream function.

Subscripts

w, wall;
∞, free stream;
$*$, denotes reference conditions;

† Present address: Center for Fluid Dynamics, Division of Engineering, Brown University, Providence, Rhode Island.

s, at the outer edge of shock layer;
0, stagnation condition in free stream (e.g. T_0), also zero-th order (no-slip) quantity;
1, first-order perturbation quantity.

I. INTRODUCTION

AN INTERESTING as well as unique feature in low Reynolds number hypersonic experimental facilities, exemplified by the Princeton hot nitrogen hypersonic wind tunnels [1], is that measurements in the laboratory can be achieved in steady-state conditions. With the advantage of long-duration testing time, measurements of wall temperature effects in low Reynolds number hypersonic flow can then be more conveniently carried out.

In this paper the classifications of the various low density hypersonic flow regimes described by Hayes and Probstein [2] are used. The Mach number and unit free stream Reynolds number in the Princeton hot nitrogen wind tunnel can be obtained at about 20 and 4×10^2 per in, respectively, so that on a 0·2 in radius sphere the flow in the stagnation region would be in the incipient merged layer regime. In this regime the viscous boundary layer begins to merge with the shock wave and there are relatively strong viscous and heat conduction effects immediately behind the shock wave. The analysis given here is concerned with this regime.

The continuum formulation of rarefied hypersonic flow was advocated in the pioneering works of Adams and Probstein [3], Probstein [4, 5] and Probstein and Kemp [6]. In the approach of the last reference, numerical integrations of the Navier–Stokes equations were carried out for highly cooled and for insulated walls after certain symmetry assumptions in the stagnation region were made and the assumption of constant density. Subsequently, Levinsky and Yoshihara [7] gave numerical results for the case when the constant density assumption was removed. Implicit in the symmetry assumptions, however, is the condition that the shock layer and shock structure must necessarily be thin compared to the body radius.

The continuum description of low Reynolds number hypersonic flow based consistently on the "thin shock layer" approximation was brought to its present stage of fruition in a series of papers by Cheng [8, 9]. For the incipient merged layer regime the problem in the shock layer is entirely independent of the shock wave structure. The conditions at the outer edge of the shock layer are those of the modified Rankine–Hugoniot relations taking into account viscous shear stress and heat conduction behind the shock wave. The effects of shock thickness and curvature do not enter into the first-order thin shock layer analysis. The shock structure can be calculated once the shock layer solution is given. With the assumption of a linear viscosity–temperature relation, the problem for the shock layer can then be exactly solved and represented in terms of known functions. The heat-transfer coefficient obtained compares well with experiments (see Cheng [8, 9], Cheng and Chang [10]). This regime of flow is also discussed by Bush [11].

The effect of increasing T_w/T_0 is to introduce slip effects at the wall and it can be considered as a perturbation of the basic no-slip solution within continuum considerations. The order of this effect has been estimated by Cheng [9] and by Cheng and Chang [12] to be $(\epsilon T_w/T_0)^{\frac{1}{2}}$, where $\epsilon \sim y_s/a \ll 1$ is the order of the shock layer thickness ratio. The effect of wall temperature on the stagnation region surface heat-transfer rate has been considered in detail by Cheng and Chang [12]. They derived a slip correction to the no-slip heat-transfer coefficient obtained earlier by Cheng [8] for the $K^2 = 0(1)$ regime. These authors also qualitatively discussed the slip effects on the shock detachment distance in the limiting case of $T_w/T_0 \to 1$.

Because of the practical interest associated with hypersonic flight and laboratory experiments in low Reynolds number hypersonic flow, the effect of wall temperature on the

behavior of the entire shock layer itself is of interest as well. The present paper complements the work of reference [12] by providing the effect of wall temperature on (1) the detailed distribution of the enthalpy function across the shock layer and (2) the shock detachment distance or the shock layer thickness.

In deriving the surface heat-transfer rate, Cheng and Chang [12] used a normal coordinate related to the stream function.† This introduces a singularity at the wall when the slip boundary conditions are applied. This difficulty was removed through the use of an inner and outer expansion technique [12]. In the present paper, the shock detachment distance and enthalpy function corrections due to slip effects will be derived through the use of the Howarth transformed normal coordinate where the problem may be considered in a similar manner to that of Lin and Schaaf [14] for the low-speed high Reynolds number stagnation region (see also Lees [15]). This is particularly advantageous in seeing physically how the slip effects affect the shock detachment distance. As a by-product the surface heat-transfer rate is obtained which verifies the low Reynolds number hypersonic stagnation region slip flow heat-transfer formula of Cheng and Chang [12] through an alternative derivation.

There are two slip effects: velocity slip and temperature jump. Their effect on the shock detachment distance is such that they tend to counteract each other. Velocity slip at the wall gives rise to an additional mass flow within the shock layer and thereby induces a mass "inflow" effect from the outer edge of the shock layer and reduces its thickness. On the other hand, the temperature jump gives rise to an additional expansion of the gas near the wall and induces an "outflow" effect which tends to thicken the shock layer. The wall temperature dependence of the "outflow" effect behaves like $(1 - T_w/T_0)\, T_w/T_0$ for a fixed rarefaction parameter K^2 in the incipient merged layer regime. This quantity has a maximum at $T_w/T_0 = \frac{1}{3}$ so that the "outflow" effect decreases as $T_w/T_0 \to 1$ when $T_w/T_0 > \frac{1}{3}$. The "inflow" effect, on the other hand, behaves like

$$k_1\left(1 - \frac{T_w}{T_0}\right)\left(\frac{T_w}{T_0}\right)^{\frac{1}{2}} + k_2\left(\frac{T_w}{T_0}\right)^{\frac{3}{2}}$$

where k_1 and k_2 are constants for a fixed rarefaction parameter in the incipient merged layer regime, and increases monotonically with T_w/T_0. This implies that, as the wall temperature increases, the "outflow" effect eventually becomes small and the "inflow" effect dominates. However, the bulk of the contribution to the shock detachment distance comes from the overall decrease of the density level in the shock layer with wall temperature.

In Section II the thin shock layer equations and boundary conditions are stated. The perturbation shock layer solution is discussed in detail in Section III, including the first-order shock layer equations and the perturbed shock and wall boundary conditions, the first-order stream function and the shock location, and the distribution of the enthalpy function across the shock layer. Section IV discusses the various corrections to the shock detachment distance. Section V discusses the relative extent of heat conduction across the entire shock layer.

II. SHOCK LAYER EQUATIONS AND BOUNDARY CONDITIONS

The thin shock layer equations obtained by Cheng [8, 9] are, for an axisymmetric blunt body in the incipient merged layer regime, in physical coordinates (see sketch in Fig. 1),

Continuity

$$\frac{\partial \rho u Z}{\partial x} + \frac{\partial \rho v Z}{\partial y} = 0 \tag{2.1}$$

Momentum

$$\rho u \frac{\partial u}{\partial x} + \rho v \frac{\partial u}{\partial y} = \frac{\partial}{\partial y}\left(\mu \frac{\partial u}{\partial y}\right) \tag{2.2}$$

† In spirit, the square root of the similarity variable used by von Kármán and Tsien [13].

$$\frac{\partial p}{\partial y} = \kappa \rho u^2 \tag{2.3}$$

Energy

$$\rho u \frac{\partial H}{\partial x} + \rho v \frac{\partial H}{\partial y} = \frac{1}{Pr} \frac{\partial}{\partial y}\left(\mu \frac{\partial H}{\partial y}\right) + \left(1 - \frac{1}{Pr}\right) \frac{\partial}{\partial y}\left(\mu \frac{\partial u^2/2}{\partial y}\right) \tag{2.4}$$

State

$$p = \rho R T. \tag{2.5}$$

We assume Pr and c_p are constants. Cheng [8, 9], however, retains the tangential pressure gradient $-\partial p/\partial x$, second order in the incipient merged layer regime, to permit uniform extension of his solution towards the higher Reynolds number range. Cheng [8, 9] also obtains, for the conditions at the outer edge of the shock layer, the modified Rankine–Hugoniot relations

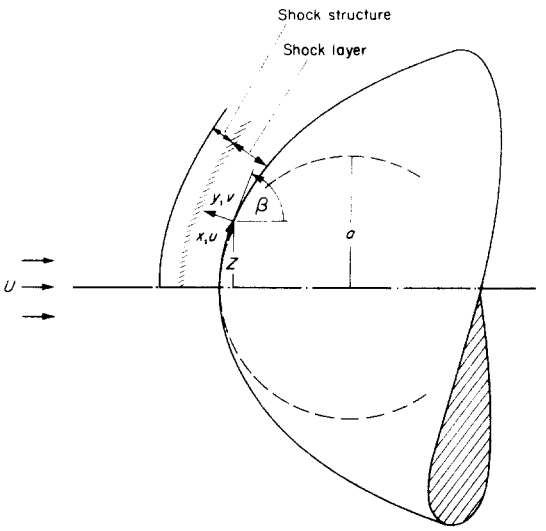

FIG. 1. Thin shock layer and notation. Schematic.

$$\left.\begin{aligned} \rho_\infty v_\infty (u - u_\infty) &= \mu \frac{\partial u}{\partial y}, \quad p = \rho_\infty v_\infty^2 \\ \rho_\infty v_\infty (H - H_\infty) &= \frac{\mu}{Pr} \frac{\partial}{\partial y}\left[H + (Pr - 1)\frac{u^2}{2}\right] \end{aligned}\right\} y = y_s \tag{2.6}$$

where $u_\infty = U \cos \beta$, $v_\infty = -U \sin \beta$. The location of the outer edge of the shock layer, y_s, is to be simultaneously determined with the solution of the shock layer problem. With the conditions at the wall given, the problem in the shock layer is then specified and can be solved independently of the shock wave structure. In the following analysis, we will be only concerned with the shock layer solution. The conditions at the wall, in terms of first-order slip effects, may be written as [16]

$$\left.\begin{aligned} u &= \frac{2 - \sigma}{\sigma} \sqrt{\left(\frac{\pi}{2}\right)} \frac{\mu}{\sqrt{(p\rho)}} \frac{\partial u}{\partial y} \\ T_b - T_w &= \frac{2\gamma}{\gamma + 1} \frac{1}{Pr} \frac{2 - \alpha}{\alpha} \sqrt{\left(\frac{\pi}{2}\right)} \frac{\mu}{\sqrt{(p\rho)}} \frac{\partial T}{\partial y} \end{aligned}\right\} y = 0 \tag{2.7}$$

where σ is Maxwell's reflection coefficient and α the thermal-accommodation coefficient. $\mu/\sqrt{(p\rho)}$ is to be evaluated at the surface gas temperature T_b which is as yet unknown. In the subsequent approximations for "small slips" within continuum considerations, however, $\mu/\sqrt{(p\rho)}$ can be evaluated at the wall temperature T_w which is here assumed to be constant.

Except for the presence of the pressure gradient normal to the surface, which does not enter in the subsequent considerations of the stagnation region, the thin shock layer equations resemble the usual compressible boundary-layer equations. Here, in general, the conditions for the outer edge are to be satisfied at the as yet to be determined shock layer edge, instead of at infinity as in the boundary-layer problem. Drawing from compressible boundary-layer theory, we introduce the Howarth–Levy transformations in the form similar to that given by Lees [17]:

$$\left.\begin{aligned} \xi &= \int \rho_0 \mu_0 u_\infty Z^2 \, dx \\ \eta &= \frac{u_\infty Z}{\sqrt{(2\xi)}} \int \rho \, dy \end{aligned}\right\} \tag{2.8}$$

With the introduction of the stream function

$$\rho u \, 2\pi Z = \frac{\partial \psi}{\partial y}, \qquad \rho v \, 2\pi Z = -\frac{\partial \psi}{\partial x} \tag{2.9}$$

and its nondimensional form

$$f = \frac{\psi}{2\pi\sqrt{(2\xi)}}, \qquad \frac{u}{u_\infty} = f' \tag{2.10}$$

the continuity equation is then automatically satisfied. The prime indicates differentiation with respect to η. With a nondimensional total enthalpy function defined as

$$\theta = \frac{H - H_w}{H_\infty - H_w} \tag{2.11}$$

the shock layer equations for the stagnation region, where $Z \sim x$, $u_\infty \sim U(x/a)$, become

$$f''' + ff'' - \tfrac{1}{2} f'^2 = 0 \tag{2.12}$$

$$p' = 0 \tag{2.13}$$

$$\theta'' + Prf\theta' = 0. \tag{2.14}$$

The linear viscosity–temperature assumption is made (i.e. $\rho\mu$ = constant). One is referred to the discussion by Cheng and Chang [10] for the justification of the assumption. The Howarth variable in the stagnation region is now reduced to

$$\eta = (\sqrt{2}) K \int \frac{\rho}{\rho_\infty} \frac{dy}{a} \tag{2.15}$$

and the rarefaction parameter K^2 is defined as

$$K^2 = \epsilon \frac{\rho_\infty U a}{\mu_0} \left(\frac{\mu_0 T_*}{\mu_* T_0} \right) \tag{2.16}$$

where μ_* is to be evaluated at the appropriate reference temperature T_* similar to that discussed in reference [10]. $K^2 = 0(1)$ for the incipient merged layer regime.

The outer boundary conditions now appear in the form

$$\left.\begin{aligned} f' &= 1 - \frac{\sqrt{2}}{K} f'' \\ \theta &= 1 - \frac{\sqrt{2}}{Pr\, K} \theta' \end{aligned}\right\} \eta = \eta_s \tag{2.17}$$

where η_s is to be simultaneously determined with the shock layer solution from the mass conservation condition $\psi = \rho_\infty U \pi x^2$. This is $[(\sqrt{2})/K] f(\eta_s) = 1$ in terms of the nondimensional stream function. The conditions at the wall are

$$\left.\begin{aligned} f &= 0 \\ f' &= \frac{2 - \sigma}{\sigma} \sqrt{\left(\epsilon \frac{\pi}{2} \frac{T_b}{T_0} \right)} \frac{\sqrt{2}}{K} f'' \\ \theta &= \frac{2\gamma}{\gamma + 1} \frac{1}{Pr} \frac{2 - \alpha}{\alpha} \sqrt{\left(\epsilon \frac{\pi}{2} \frac{T_b}{T_0} \right)} \frac{\sqrt{2}}{K} \theta' \end{aligned}\right\} \tag{2.18}$$

III. PERTURBATION SHOCK LAYER SOLUTION

A. *First-order shock layer equations*

Within the thin shock layer continuum description of low Reynolds number hypersonic flow, the effect of velocity slip and temperature jump can be treated as a perturbation on the no-slip solution. Since the slip effects are of order $\sqrt{\epsilon}$, one then expands as follows:

$$f = f_0 + (\sqrt{\epsilon}) f_1 + \ldots \tag{3.1}$$

$$\theta = \theta_0 + (\sqrt{\epsilon}) \theta_1 + \ldots \tag{3.2}$$

where the zero-th order functions are Cheng's

[8] no-slip stagnation region shock layer solution. Since the zero-th order functions [8] appear repeatedly in the first-order problem, they are quoted in Appendix A for the purpose of reference.

The first-order perturbation shock layer equations are obtained by substituting the expansions, equations (3.1) and (3.2), into equations (2.12) and (2.14), retaining terms only of the first order

$$f_1''' + f_0 f_1'' - f_0' f_1' + f_0'' f_1 = 0 \quad (3.3)$$

$$\theta_1'' + Pr f_0 \theta_1' = -Pr\,\theta_0' f_1. \quad (3.4)$$

With Cheng's [8] stream function f_0, stated in Appendix A, the first-order momentum equation, (3.3), then becomes

$$f_1''' + C(\eta^2 f_1'' - 2\eta f_1' + 2f_1) = 0. \quad (3.5)$$

Upon substituting Cheng's [8] enthalpy function θ_0, also stated in Appendix A, the first-order energy equation (3.4) becomes

$$\theta_1'' + Pr\,C\eta^2\theta_1' = -Pr\{(Pr\,KC_{H_0}/\sqrt{2}) \times \exp[-k(\eta/\eta_{s_0})^3]\} f_1. \quad (3.6)$$

B. *First-order shock and wall boundary conditions*

Although the exact location of the outer edge of the shock layer is as yet unknown, it may be written as the following expansion

$$\eta_s = \eta_{s_0} + (\sqrt{\epsilon})\,\eta_{s_1} + \ldots \quad (3.7)$$

where η_{s_1} is the first-order shock location perturbation, to be determined as part of the solution. The first-order shock boundary conditions are obtained by substituting the expansions, equations (3.1) and (3.2), into equation (2.17) and subsequently transferring the location where the conditions are to be applied from η_s to η_{s_0} by a Taylor expansion.

The shock boundary condition for f_1 is then

$$\left.\begin{aligned} f_1' + [(\sqrt{2})/K] f_1'' &= -\eta_{s_1}\{f_0'' + [(\sqrt{2})/K] f_0'''\} \\ &= -\eta_{s_1} 2C \end{aligned}\right\} \eta = \eta_{s_0}. \quad (3.8)$$

The corresponding condition for θ_1 is

$$\left.\begin{aligned} \theta_1 + [(\sqrt{2})/Pr\,K]\,\theta_1' &= -\eta_{s_1}\{\theta_0' + [(\sqrt{2})/(Pr\,K)]\theta_0''\} \\ &= 0 \end{aligned}\right\} \eta = \eta_{s_0}. \quad (3.9)$$

The right side of equation (3.9) becoming zero can be easily shown by substituting $\theta_0'' = -Pr\,f_0\theta_0'$ from Cheng's [8] energy equation and subsequently noting that the zero-th order stream function is required to be $[(\sqrt{2})/K] f_0 = 1$ at $\eta = \eta_{s_0}$ from mass conservation considerations.

The boundary conditions at the wall are now

$$\left.\begin{aligned} f_1 &= 0 \\ f_1' &= \frac{2-\sigma}{\sigma}\sqrt{\left(\frac{\pi}{2}\frac{T_w}{T_0}\right)}\frac{\sqrt{2}}{K} f_0'' = \frac{2-\sigma}{\sigma}\sqrt{\left(\frac{\pi}{2}\frac{T_w}{T_0}\right)}\frac{\sqrt{2}}{K} 2C \end{aligned}\right\} \eta = 0 \quad (3.10)$$

and

$$\theta_1 = \frac{2\gamma}{\gamma+1}\frac{1}{Pr}\frac{2-\alpha}{\alpha}\sqrt{\left(\frac{\pi}{2}\frac{T_w}{T_0}\right)}\frac{\sqrt{2}}{K}\theta_0' = \frac{2\gamma}{\gamma+1}\frac{2-\alpha}{\alpha}\sqrt{\left(\frac{\pi}{2}\frac{T_w}{T_0}\right)} C_{H_0}\Big\} \eta = 0. \quad (3.11)$$

C. *First-order stream function and shock location*

The first-order momentum equation, given by equation (3.5), has the exact solution (see, for instance, Kamke [18])

$$f_1 = a_1\eta + a_2\eta^2 + a_3\{\eta \int_0 \eta^{-2} \exp[-C\eta^3/3]\mathrm{d}\eta - \eta^2 \int_0 \eta^{-3} \exp[-C\eta^3/3]\,\mathrm{d}\eta\} \quad (3.12)$$

where a_1, a_2 and a_3 are constants to be determined. The fact that a_3 must vanish in order to satisfy the first of equations (3.10) may be seen by evaluating the integrals by parts once to bring out the finite contribution at $\eta = 0$. The third term in equation (3.12) becomes

$$a_3\left\{\tfrac{1}{2}\left(\frac{C\eta^3}{3}\right)^{\frac{1}{3}}\gamma\left(\tfrac{1}{3},\frac{C\eta^3}{3}\right) - \left(\frac{C\eta^3}{3}\right)^{\frac{1}{3}}\gamma\left(\tfrac{2}{3},\frac{C\eta^3}{3}\right) - \tfrac{1}{2}\exp(-C\eta^3/3)\right\}.$$

Both incomplete gamma functions vanish at $\eta = 0$, while the exponential term gives a contribution of $-\frac{1}{2}$. Hence $a_3 = 0$.

The second condition in equation (3.10) gives

$$a_1 = \frac{2-\sigma}{\sigma}\sqrt{\left(\frac{\pi}{2}\frac{T_w}{T_0}\right)}\frac{\sqrt{2}}{K}2C. \tag{3.13}$$

The shock boundary condition, equation (3.8), gives

$$a_2 = -(a_1 + \eta_{s_1}2C)/2\,[(\sqrt{2})/K + \eta_{s_0}]. \tag{3.14}$$

The solution for the first-order stream function, f_1, still contains the unknown η_{s_1} which is to be presently determined. At the outer edge of the shock layer η_s, we recall from the previous discussion in Section II that the nondimensional stream function is required to be $[(\sqrt{2})/K]\,f(\eta_s) = 1$. In terms of the first-order quantities, after transferring the application of this condition from $\eta_s = \eta_{s0} + (\sqrt{\epsilon})\,\eta_{s_1} + \ldots$ to η_{s_0}, we have

$$\eta_{s_1} f_0' + f_1 = 0 \qquad \text{at} \quad \eta = \eta_{s_0}. \tag{3.15}$$

Substituting equation (3.14) into equation (3.12) (with $a_3 = 0$) for f_1, equation (3.15) then determines η_{s_1} as

$$\eta_{s_1} = -a_1/2C \tag{3.16}$$

where a_1 is given by equation (3.13). Upon substituting η_{s_1} back into the solution for f_1, equation (3.14) then gives the condition that $a_2 = 0$. Finally

$$f_1 = \left[\frac{2-\sigma}{\sigma}\sqrt{\left(\frac{\pi}{2}\frac{T_w}{T_0}\right)}\frac{\sqrt{2}}{K}2C\right]\eta. \tag{3.17}$$

A useful form of η_{s_1} is the ratio η_{s_1}/η_{s_0}, which may be written in the form

$$\frac{\eta_{s_1}}{\eta_{s_0}} = -\frac{2-\sigma}{\sigma}\sqrt{\left(\frac{\pi}{2}\frac{T_w}{T_0}\right)\left(\frac{Pr}{3k}\right)}. \tag{3.18}$$

The physical reason for η_{s_1} being negative is that the additional mass flow near the wall due to tangential velocity slip induces an inflow of mass across the outer edge of the shock layer, and this has the direct effect of reducing the shock layer thickness.

D. *First-order enthalpy function*

The nonhomogeneous first-order energy equation, (3.6), can be integrated directly to give

$$\theta_1 = -Pr(Pr\,KC_{H_0}/\sqrt{2})\int_0^{\eta}\exp\left[-k(\bar{\eta}/\eta_{s_0})^3\right] \times \int_0^{\bar{\eta}} f_1(\eta')\,d\eta'\,d\bar{\eta} + b_1\int_0^{\eta}\exp\left[-k(\bar{\eta}/\eta_{s_0})^3\right]d\bar{\eta} + b_2. \tag{3.19}$$

With f_1 given by equation (3.17), equation (3.19) can then be put into the form

$$\theta_1 = -\frac{2-\sigma}{\sigma}\sqrt{\left(\frac{\pi}{2}\frac{T_w}{T_0}\right)}Pr\,C_{H_0} \times \{1 - \exp\left[k(\eta/\eta_{s_0})^3\right]\} + b_1\frac{\sqrt{2}}{Pr\,K}k^{\frac{1}{3}}\gamma\left[\frac{1}{3}, k\left(\frac{\eta}{\eta_{s_0}}\right)^3\right] + b_2. \tag{3.20}$$

From the shock boundary condition for θ_1 given by equation (3.9), b_1 is determined as

$$b_1 = \frac{2-\sigma}{\sigma}\sqrt{\left(\frac{\pi}{2}\frac{T_w}{T_0}\right)}Pr \times C_{H_0}\left(1 - \frac{1}{Pr}\frac{2\gamma}{\gamma+1}\frac{2-\alpha\sigma}{2-\sigma\alpha}\right) \times \left(\frac{Pr\,K}{\sqrt{2}}C_{H_0}\right). \tag{3.21}$$

This form is obtained through the use of the definition of Cheng's [8] heat-transfer coefficient C_{H_0}, quoted in Appendix A.

The wall boundary condition, equation (3.11), determines b_2 as

$$b_2 = \frac{2\gamma}{\gamma+1}\frac{2-\alpha}{\alpha}\sqrt{\left(\frac{\pi}{2}\frac{T_w}{T_0}\right)}C_{H_0}. \quad (3.22)$$

Through the use of Cheng's [8] enthalpy function θ_0 (and θ_0'), the first-order enthalpy profile given by equations (3.20), (3.21) and (3.22) can be written entirely in terms of the zero-th order functions

$$\theta_1(\eta) = \frac{2-\sigma}{\sigma}\sqrt{\left(\frac{\pi}{2}\frac{T_w}{T_0}\right)}Pr\left\{\frac{\sqrt{2}}{Pr\,K}\theta_0'(\eta) + C_{H_0}\left(\frac{1}{Pr}\frac{2\gamma}{\gamma+1}\frac{2-\alpha}{2-\sigma}\frac{\sigma}{\alpha}-1\right)\times[1-\theta_0(\eta)]\right\}. \quad (3.23)$$

To illustrate the effect of wall-temperature ratio on the over-all enthalpy function across the shock layer, Figs. 2, 3 and 4 are presented for the values of rarefaction parameter $K^2 = 10$, 4 and 1, respectively. The normal coordinate is η/η_{s_0}. For a fixed value of K^2, increasing the wall temperature increases the value of the enthalpy function from its no-slip value θ_0. This effect is more pronounced near the wall.

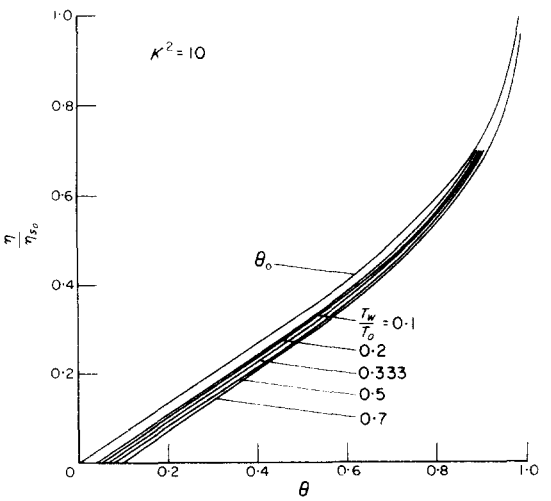

FIG. 2. Enthalpy function as function of η/η_{s_0}, for $K^2 = 10$, $\gamma = 1{\cdot}4$, $Pr = 0{\cdot}71$, $\sigma = \alpha = 1$ and various values of T_w/T_0.

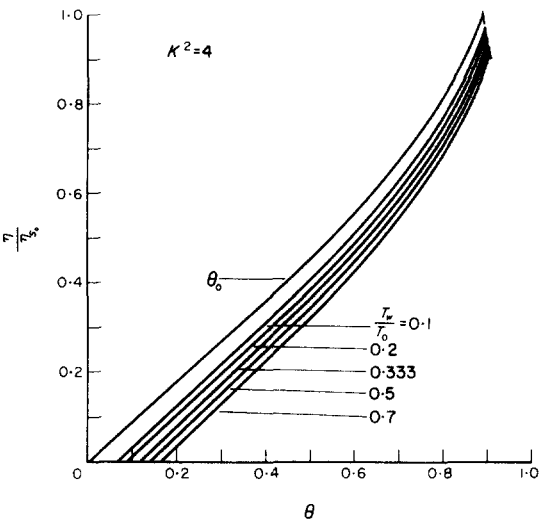

FIG. 3. Enthalpy function as function of η/η_{s_0}, for $K^2 = 4$, $\gamma = 1{\cdot}4$, $Pr = 0{\cdot}71$, $\sigma = \alpha = 1$ and various values of T_w/T_0.

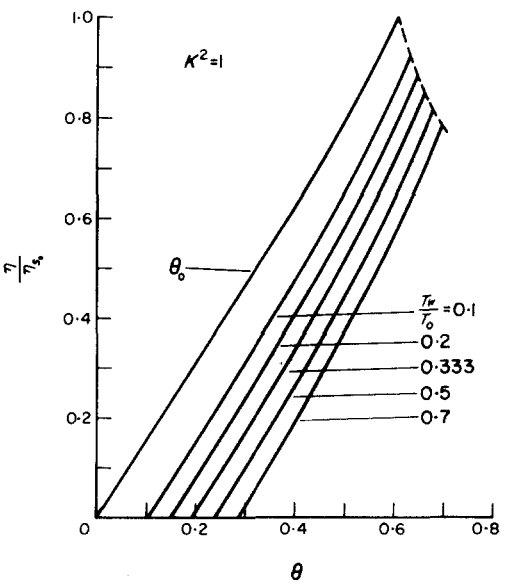

FIG. 4. Enthalpy function as function of η/η_{s_0}, for $K^2 = 1$, $\gamma = 1{\cdot}4$, $Pr = 0{\cdot}71$, $\sigma = \alpha = 1$ and various values of T_w/T_0.

At the same time the outer edge of the shock layer is brought closer to the wall due to the effect of velocity slip. For a fixed wall-temperature ratio, the distortion of the no-slip enthalpy function becomes more pronounced as K^2 decreases.

E. *Relation between physical and transformed coordinates*

The relation between the physical coordinate y and the transformed coordinate η is obtained by inverting the Howarth transformation. Its form for the stagnation region is defined by equation (2.15). Since the pressure is constant across the shock layer at the stagnation region, the density ratio ρ_0/ρ is simply T/T_0. The latter is simply related to the enthalpy function θ in the stagnation region. The physical distance normal to the wall is then obtained from the integral

All the first-order "inflow" correction is embedded in the integration of the first two terms in equation (3.24) with respect to η over the interval $0 \leqslant \eta \leqslant \eta_{s_0} + (\sqrt{\epsilon})\eta_{s_1}$. The functions resulting from this integration are further expanded in a Taylor series about η_{s_0}. To be consistent only the first-order perturbations need to be retained. The zero-th order functions resulting from such an expansion would be the basic contribution to the shock detachment distance obtained from Cheng's [8] solution.

$$\frac{y}{\epsilon a} = \frac{1}{(\sqrt{2})K}\int_0^{\eta}\left\{\frac{T_w}{T_0} + \left(1 - \frac{T_w}{T_0}\right)[\theta_0(\bar{\eta}) + (\sqrt{\epsilon})\,\theta_1(\bar{\eta}) + \ldots]\right\} d\bar{\eta}\ . \tag{3.24}$$

For brevity, we define $\zeta = \eta/\eta_{s_0}$. The physical coordinate is then obtained as

$$\frac{K^2 Pr}{3k}\frac{y}{\epsilon a} = \frac{T_w}{T_0}\zeta + \left(1 - \frac{T_w}{T_0}\right)[\zeta\theta_0(\zeta) - k^{\frac{1}{3}}C_{H_0}\gamma(\tfrac{2}{3}, k\zeta^3)]$$
$$+ \frac{2-\sigma}{\sigma}\sqrt{\left(\epsilon\frac{\pi}{2}\frac{T_w}{T_0}\right)}\left(1 - \frac{T_w}{T_0}\right)Pr\left\{\frac{1}{3k}\theta_0(\zeta) + C_{H_0}\left(\frac{1}{Pr}\frac{2\gamma}{\gamma+1}\frac{2-\alpha\sigma}{2-\sigma\alpha} - 1\right)(\zeta[1 - \theta_0(\zeta)]\right.$$
$$\left. + k^{\frac{1}{3}}\gamma(\tfrac{2}{3}, k\zeta^3))\right\}. \tag{3.25}$$

Again, use is made of the definition of Cheng's [8] enthalpy function θ_0.

IV. SHOCK DETACHMENT DISTANCE

The shock detachment distance is obtained by carrying the integral in equation (3.24) to the perturbed edge of the shock layer $\eta_s = \eta_{s_0} + (\sqrt{\epsilon})\eta_{s_1} + \ldots$.

The first-order functions, linear in $\sqrt{\epsilon}$, are then the actual "inflow" correction terms. The integration of the third term in equation (3.24), up to η_{s_0} only, gives the "outflow" correction terms.

For the purpose of keeping the various contributions to the shock detachment distance distinct as discussed above, we may write

$$\frac{y_s}{\epsilon a} = \frac{y_{s_0}}{\epsilon a} + (\sqrt{\epsilon})\left(\frac{y_{s_1}}{\epsilon a}\right)_{\text{Inflow}} + (\sqrt{\epsilon})\left(\frac{y_{s_1}}{\epsilon a}\right)_{\text{Outflow}} + \ldots\ . \tag{4.1}$$

The three functions on the right of equation (4.1) are then defined as:

(1) The zero-th order contribution is the shock detachment distance given by Cheng [8] for the no-slip case

$$\frac{y_{s_0}}{\epsilon a} = \frac{3k}{Pr\,K^2}\left\{\frac{T_w}{T_0} + \left(1 - \frac{T_w}{T_0}\right)k^{\frac{1}{3}}\,C_{H_0}[\gamma(\tfrac{1}{3}, k) - k^{-\frac{1}{3}}\gamma(\tfrac{2}{3}, k)]\right\}. \tag{4.2}$$

(2) The "inflow" correction, due to velocity slip, is

$$(\sqrt{\epsilon})\left(\frac{y_{s_1}}{\epsilon a}\right)_{\text{Inflow}} = -\sqrt{\left(\epsilon\frac{\pi}{2}\right)\frac{2-\sigma}{\sigma}\frac{1}{K^2}}\left\{\left(\frac{T_w}{T_0}\right)^{\frac{3}{2}} + \left(1-\frac{T_w}{T_0}\right)\left(\frac{T_w}{T_0}\right)^{\frac{1}{2}} k^{\frac{2}{3}} C_{H_0}\gamma(\tfrac{1}{3}, k)\right\}. \tag{4.3}$$

(3) The "outflow" correction, due to temperature jump, is

$$(\sqrt{\epsilon})\left(\frac{y_{s_1}}{\epsilon a}\right)_{\text{Outflow}} = +\sqrt{\left(\epsilon\frac{\pi}{2}\right)\frac{2-\sigma}{\sigma}\frac{3k}{K^2}C_{H_0}}\left(1-\frac{T_w}{T_0}\right)\left(\frac{T_w}{T_0}\right)^{\frac{1}{2}}\left\{\frac{1}{3k^{\frac{1}{3}}}\gamma(\tfrac{1}{3}, k)\right.$$
$$\left. + \left(\frac{1}{Pr}\frac{2\gamma}{\gamma+1}\frac{2-\alpha}{2-\sigma}\frac{\sigma}{\alpha} - 1\right)(1 - k^{\frac{2}{3}} C_{H_0}[\gamma(\tfrac{1}{3}, k) - k^{-\frac{1}{3}}\gamma(\tfrac{2}{3}, k)])\right\}. \tag{4.4}$$

The negative of $(\sqrt{\epsilon})(y_{s_1}/\epsilon a)_{\text{Inflow}}$ is shown in Fig. 5 as solid lines as a function of T_w/T_0 for various values of K^2, while $(\sqrt{\epsilon})(y_{s_1}/\epsilon a)_{\text{Outflow}}$ is shown in the same figure as dotted lines. The "inflow" correction is monotonic and always tends to decrease the shock detachment distance. The "outflow" correction always give a positive contribution and has a maximum at $T_w/T_0 = 0{\cdot}333$, beyond which it decreases. The difference between the solid and dotted curves for a fixed

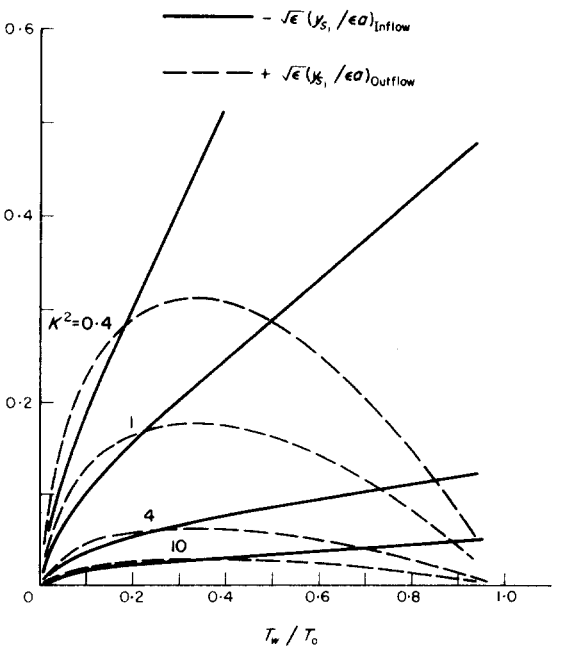

FIG. 5. Shock detachment distance "inflow" and "outflow" corrections as function of wall-temperature ratio, for $\gamma = 1{\cdot}4$, $Pr = 0{\cdot}71$, $\sigma = \alpha = 1$ and various values of K^2.

K^2 gives the net correction to the zero-th order no-slip shock detachment distance. For the range of K^2 shown in Fig. 5, the net correction to the shock detachment distance is positive for the lower range of wall temperature ratios ($T_w/T_0 \lesssim 0{\cdot}2$) and is negative beyond this range ($T_w/T_0 \gtrsim 0{\cdot}2$).

The dotted lines in Fig. 6 show the zero-th order no-slip shock detachment distance obtained by Cheng [8], $(y_{s_0}/\epsilon a)$, as a function of the rarefaction parameter for various wall-temperature ratios. The solid lines are the new shock detachment distances with the slip corrections applied. For the lower ranges of wall-temperature ratios $(y_{s_0}/\epsilon a)$ tends to increase with K^2, while the corrections give a net positive contribution. For relatively higher ranges of wall-temperature ratios $(y_{s_0}/\epsilon a)$ tends to decrease with K^2, while the corrections give a net negative contribution. Hence the corrected shock detachment distance tends to remain constant with K^2 as shown in Fig. 6. At $K^2 = 1$, for instance, $(y_s/\epsilon a)$ at $T_w/T_0 \sim 0{\cdot}5$ is about twice its value at $T_w/T_0 \to 0$, that is, $y_s/(y_s)_{T_w/T_0 \to 0} \sim 2$. This is certainly an experimentally observable ratio.

V. HEAT CONDUCTION ACROSS SHOCK LAYER

The extent of heat conduction across the entire shock layer is of interest in the incipient merged layer regime. In particular, this consideration will give the slip effects, if any, on the relative extent of heat conduction into the shock layer at the outer edge of the shock layer as compared to heat conduction into the wall.

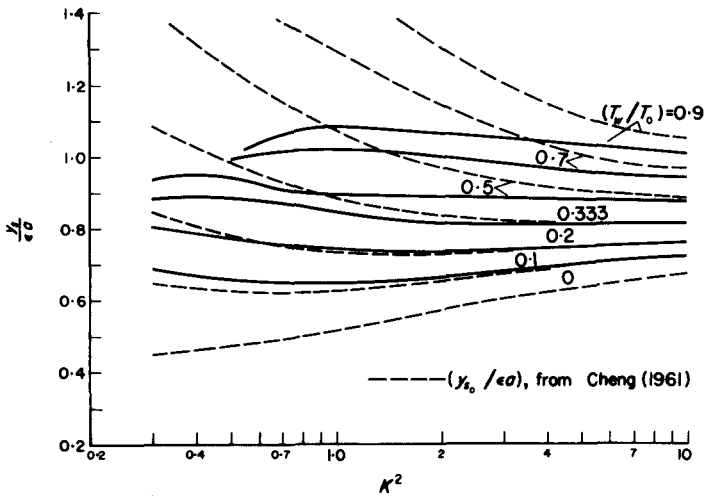

FIG. 6. Shock detachment distance as function of rarefaction parameter, for $\gamma = 1{\cdot}4$, $Pr = 0{\cdot}71$, $\sigma = \alpha = 1$ and various values of T_w/T_0.

The following nondimensional ratio is written for any point across the shock layer:

$$\frac{[k(\partial T/\partial y)]}{\rho_\infty U(H_\infty - H_w)} = \frac{\sqrt{2}}{Pr\,K}\theta_0'(\eta)\left\{1 - \sqrt{\left(\epsilon\frac{\pi}{2}\frac{T_w}{T_0}\right)Pr\frac{2-\sigma}{\sigma}}\left[\left(\frac{\eta}{\eta_{s_0}}\right)^2 + \left(\frac{1}{Pr}\frac{2\gamma}{\gamma+1}\frac{2-\alpha}{2-\sigma}\frac{\sigma}{\alpha} - 1\right)C_{H_0}\right] + \ldots\right\}$$

$$\simeq \frac{C_{H_0}\exp\left[-k(\eta/\eta_{s_0})^3\right]}{1 + \sqrt{\left(\epsilon\frac{\pi}{2}\frac{T_w}{T_0}\right)Pr\frac{2-\sigma}{\sigma}}\left[\left(\frac{\eta}{\eta_{s_0}}\right)^2 + \left(\frac{1}{Pr}\frac{2\gamma}{\gamma+1}\frac{2-\alpha}{2-\sigma}\frac{\sigma}{\alpha} - 1\right)C_{H_0}\right]} \tag{5.1}$$

where use is made of equation (3.23) and the definition of $\theta_0'(\eta)$.

At the wall equation (5.1) becomes

$$C_H \equiv \frac{[k(\partial T/\partial y)]_w}{\rho_\infty U(H_\infty - H_w)} \simeq \frac{C_{H_0}}{1 + \sqrt{\left(\epsilon\frac{\pi}{2}\frac{T_w}{T_0}\right)Pr\frac{2-\sigma}{\sigma}}\left(\frac{1}{Pr}\frac{2\gamma}{\gamma+1}\frac{2-\alpha}{2-\sigma}\frac{\sigma}{\alpha} - 1\right)C_{H_0}} \tag{5.2}$$

which is the corresponding surface heat-transfer formula obtained by Cheng and Chang [12]. Hence their wall heat-transfer result is verified by an alternate method of derivation.

At the outer edge of the perturbed shock layer, equation (5.1) can be appropriately approximated by expansion about η_{s_0} as was done before. After performing this expansion, we then form the ratio of equation (5.1) at $\eta_s = \eta_{s_0} + (\sqrt{\epsilon})\eta_{s_1} + \ldots$ to its corresponding value at the wall, equation (5.2). This then gives the ratio of heat conducted into the shock layer behind the shock wave to the heat conducted into the wall,

$$\frac{\dot{q}_s}{\dot{q}_w} = \frac{(\dot{q}_s)_0}{(\dot{q}_w)_0} = \exp(-k). \tag{5.3}$$

We thus arrive at the simple result that this ratio is the same as the corresponding ratio

when slip effects are absent. That is, it is independent of the wall temperature ratio. It only depends on the rarefaction parameter K^2 and the Prandtl number Pr through the parameter k.

ACKNOWLEDGEMENTS

This study was partially supported by the Office of Aerospace Research, United States Air Force, Contract AF 49(638)-1271, under the monitorship of Major R. C. Smith of the Aerospace Research Laboratory, Wright–Patterson Air Force Base and by the National Science Foundation under Grant NSF GK-59.

I wish to thank Professor S. H. Lam for suggesting the study and for subsequent helpful discussions. The encouragement and interest of Professor S. M. Bogdonoff is gratefully acknowledged. The numerous comments of Dr. P. A. Sullivan were very much appreciated. I am especially indebted to Professor H. K. Cheng of the University of Southern California for his critical reading and comments on an earlier draft of the manuscript.

REFERENCES

1. I. E. Vas and G. Koppenwallner, The Princeton University high pressure hypersonic nitrogen tunnel N-3. Princeton University Department of Aerospace and Mechanical Sciences Report 690 (1964).
2. W. D. Hayes and R. F. Probstein, *Hypersonic Flow Theory*. Academic Press, New York (1959).
3. M. C. Adams and R. F. Probstein, On the validity of continuum theory for satellite and hypersonic flight problems at high altitudes, *Jet Propul.* **28**, 86 (1958).
4. R. F. Probstein, Continuum theory and rarefied, hypersonic aerodynamics, in *Rarefied Gas Dynamics* edited by F. M. Devienne, p. 416. Pergamon Press, London (1960).
5. R. F. Probstein, Aerodynamics of rarefied gases, in *Rarefied Gas Dynamics*, edited by F. M. Devienne, p. 262. Pergamon Press, London (1960).
6. R. F. Probstein and N. Kemp, Viscous aerodynamic characteristics in hypersonic rarefied gas flow, *J. Aerospace Sci.* **27**, 174 (1960).
7. E. S. Levinsky and H. Yoshihara, Rarefied hypersonic flow over a sphere, in *Hypersonic Flow Research*, edited by F. R. Riddell, p. 81. Academic Press, New York (1962).
8. H. K. Cheng, Hypersonic shock-layer theory of the stagnation region at low Reynolds number, in *Proceedings of the* 1961 *Heat Transfer and Fluid Mechanics Institute*, p. 161. Stanford University Press, Palo Alto (1961).
9. H. K. Cheng, The blunt-body problem in hypersonic flow at low Reynolds number. Cornell Aeronautical Laboratory Report No. AF-1285-A-10 (1963).
10. H. K. Cheng and A. L. Chang, Remarks on stagnation region in rarefied high Mach-number flow, *AIAA Jl* **1**, 231 (1963).
11. W. B. Bush, On the viscous hypersonic blunt-body problem, *J. Fluid Mech.* **20**, 353 (1964).
12. H. K. Cheng and A. L. Chang, Bow-shock structure and slip effects in low-density hypersonic flow. Aerospace Research Laboratory Report 64-26 (1964).
13. Th. von Kármán and H. S. Tsien, Boundary layer in compressible fluids. *J. Aeronaut. Sci.* **5**, 227 (1938).
14. T. C. Lin and S. A. Schaaf, Effect of slip on flow near a stagnation point and in a boundary layer. NACA TN 2568 (1951).
15. L. Lees, Recent developments in hypersonic flow. *Jet Propul.* **27**, 1162 (1957).
16. S. A. Schaaf and P. L. Chambré, Flow of rarefied gases. in *Fundamentals of Gas Dynamics*, edited by H. W. Emmons, p. 687. Princeton University Press, Princeton (1958).
17. L. Lees, Laminar heat transfer over blunt-nosed bodies at hypersonic flight speeds, *Jet Propul.* **26**, 259 (1956).
18. E. Kamke, *Differentialgleichungen Lösungsmethoden und Lösungen*, 3rd edn., S. 512. Chelsea, New York (1959).
19. A. Erdélyi, W. Magnus, F. Oberhettinger and F. G. Tricomi, *Higher Transcendental Functions*, Vol. II, Bateman Manuscript Project, p. 133. McGraw-Hill, New York (1953).
20. M. Abramowitz, Table of the integral $\int_0^x \exp(-u^3)\,du$, *J. Math. Phys.* **30**, 162 (1951).

APPENDIX A [8, 9]

The zero-th order problem, which is Cheng's [8, 9] no-slip solution for the stagnation region when the rarefaction parameter K^2 is of order unity, is quoted here for the purpose of convenience. The zero-th order and related functions appear repeatedly in the perturbation solution for slip effects.

The governing transformed equations are

$$f_0''' + f_0 f_0'' - \tfrac{1}{2}(f_0')^2 = 0$$

$$\theta_0'' + Pr\, f_0 \theta_0' = 0.$$

The shock boundary conditions are

$$\left.\begin{aligned} f_0' &= 1 - [(\sqrt{2})/K]\, f_0'' \\ \theta_0 &= 1 - [(\sqrt{2})/Pr\, K]\, \theta_0' \end{aligned}\right\} \eta = \eta_{s_0}$$

and the wall boundary conditions are $f_0 = f_0' = \theta_0 = 0$ at $\eta = 0$. The solutions are

$$f_0 = C\eta^2$$

$$\theta_0 = k^{\frac{1}{3}} C_{H_0}\, \gamma[\tfrac{1}{3}, k(\eta/\eta_{s_0})^3],$$

where the heat-transfer coefficient is

$$C_{H_0} = [(\sqrt{2})/Pr\, K]\, \theta_0'(0)$$

$$= [k^{\frac{1}{3}}\gamma(\tfrac{1}{3}, k) + \exp(-k)]^{-1}$$

and

$$C = [(\sqrt{2})K^3/16]\{\sqrt{[(4/K^2) + 1]} - 1\}^2$$

$$k = (2Pr/3)\{\sqrt{[(4/K^2) + 1]} - 1\}^{-1}.$$

The outer edge of the zero-th order shock layer is given by

$$\eta_{s_0} = \left[\frac{K}{(\sqrt{2})C}\right]^{\frac{1}{4}}.$$

The function appearing in θ_0 and C_{H_0} is the incomplete gamma function of order $\frac{1}{3}$. Its general form is defined as [19]

$$\gamma(a, \chi) = \int_0^{\chi} \exp(-t)\, t^{a-1}\, dt \qquad (a > 0)$$

which is of order a and of argument χ. It is noted that in the special case of order $\frac{1}{3}$, the related integral

$$I(\chi^{\frac{1}{3}}) = \tfrac{1}{3}\gamma(\tfrac{1}{3}, \chi) = \int_0^{\chi} \exp(-t^3)\, dt$$

has been directly calculated and tabulated by Abramowitz [20].

NOTE ADDED IN PROOF

A review as well as discussion of extensions and applications of various approaches to continuum hypersonic rarefied-gas dynamics is given in the recent paper of H. K. Cheng, Viscous hypersonic blunt-body problems and the Newtonian theory, in *Proceedings of International Symposium on Fundamental Phenomena in Hypersonic Flow*, edited by J. G. Hall, p. 90. Cornell University Press, Ithaca (1966).

Résumé—On décrit l'effet de la température pariétale sur le comportement de la couche de choc hypersonique au point d'arrêt dans le cas de l'écoulement de début de jonction des couches. Le profil d'enthalpie à travers la couche de choc est obtenu. On montre que la distance de détachement du choc est sujette à des corrections compensatrices d'un effet d'"aspiration" due au glissement et d'un effet de "soufflage" dû au saut de température, la contribution principale venant de la diminution globale de densité due au chauffage de la paroi. La correction totale rend la distance de détachement du choc relativement constante lorsque K^2 varie, où K^2 est le paramètre de raréfaction de Cheng, la température pariétale étant fixée. Le rapport du flux de chaleur derrière l'onde de choc à celui à la paroi est indépendant de la température pariétale et ne varie pratiquement pas lorsque les effets de glissement sont absents.

Zusammenfassung—Es wird der Einfluss der Wandtemperatur auf das Verhalten der Stoss-Schicht in einem hypersonischen Staugebiet bei beginnender gemischter Schichtströmung beschrieben. Man erhält das Enthalpieprofil über die Stoss-Schicht. Es zeigt sich, dass der Abstand des abgelösten Stosses von der Wand zwei ausgleichenden Korrekturen unterworfen ist, einem "Zufluss"-Effekt durch Geschwindigkeitsgleitung und einem "Abfluss"-Effekt durch Temperatursprung, wobei der Hauptbeitrag aus der Gesamtdichteabnahme durch Wandheizung kommt. Die gesamten Korrekturen ergeben, dass der Abstand des abgelösten Stosses an der Wand für eine feste Wandtemperatur relative konstant in Bezug auf K^2 bleibt, wobei K^2 Chengs Verdünnungsfaktor ist. Das Verhältnis der Wärmestromdichte hinter der Stosswelle zur Wärmestromdichte an der Wand erweist sich als unabhängig von der Wandtemperatur und ist im wesentlichen gleich dem entsprechenden Verhältnis, wenn Gleiteffekte nicht vorhanden sind.

Аннотация—Описывается влияние температуры стенки на поведение гиперзвукого ударного слоя вблизи критической точки в режиме перемешивания. Получено распределение энтальпии поперек ударного слоя. Показано, что при расчете отрыва скачка уплотнения необходимо учитывать поправки за счет «притока» из-за скольжения скорости и «оттока», вызванного температурным скачком, при чем преобладающим является снижение общей плотности из-за нагрева стенки. С учетом всех поправок установлено, что место отрыва скачка уплотнения остается неподвижным при неизменном K для постоянной температуры стенки, где K параметр разрежения Ченга. Покае зано, что отношение теплового потока за ударной волной к тепловому потоку на стенке не зависит от температуры стенки и не отличается от соответствующего отношения при отсутствии скольжения.